ResearchGate

See discussions, stats, and author profiles for this publication at: https://www.researchgate.net/publication/51167709

# Unusually Large Magnetic Anisotropy in Electrochemically Deposited Co-Rich Co-Pt Films

**ARTICLE** *in* ACS APPLIED MATERIALS & INTERFACES · JUNE 2011

Impact Factor: 6.72 · DOI: 10.1021/am200267u · Source: PubMed

CITATIONS
2

READS
27

**8 AUTHORS**, INCLUDING:

P.L. Cavallotti
Politecnico di Milano
**171** PUBLICATIONS **1,372** CITATIONS
SEE PROFILE

Mario Italo Trioni
Italian National Research Council
**89** PUBLICATIONS **678** CITATIONS
SEE PROFILE

Available from: P.L. Cavallotti
Retrieved on: 03 February 2016

ACS APPLIED MATERIALS & INTERFACES

LETTER

www.acsami.org

# Unusually Large Magnetic Anisotropy in Electrochemically Deposited Co-Rich Co−Pt Films

V. Sirtori,[†] P. L. Cavallotti,[†] R. Rognoni,[‡] X. Xu,[§,∥] G. Zangari,[*,§] G. Fratesi,[⊥] M. I. Trioni,[⊥,#] and M. Bernasconi[⊥]

[†]Dipartimento di Chimica, Materiali e Ingegneria Chimica, Politecnico di Milano, via Mancinelli 7, 20131 Milano, Italy,

[‡]SEM srl - Services for Electronic Manufacturing, Via Lecco 61, 20059 Vimercate (MB), Italy,

[§]Department of Materials Science and Engineering and CESE, University of Virginia, Charlottesville, Virginia 22904, United States

[⊥]Department of Materials Science, University of Milano-Bicocca, Via R. Cozzi 53, 20125 Milano, Italy

Supporting Information

**ABSTRACT:** Co-rich Co−Pt films grown by electrodeposition from an amino-nitrite/citrate/glycine electrolyte onto Au(111) substrates apparently grow with a hexagonal structure, with its *c*-axis directed perpendicular to the surface. The films exhibit a perpendicular magnetic anisotropy (MCA) of the same order of magnitude as the shape anisotropy. Experimental estimates of the MCA result in a higher anisotropy than that reported for bulk materials of the same composition, but similar to values measured in films grown by vacuum methods at relatively high temperature, which partly consist of a high anisotropy, metastable orthorhombic *Pmm*2 phase. Comparison of valence band X-ray photoelectron spectroscopy measurements on electrodeposited films with density functional theory simulations of the electronic structure of the various reported $Co_3Pt$ structures support the notion that the films may consist of a mixture of the hexagonal and the *Pmm*2 structure.

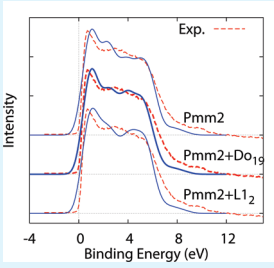


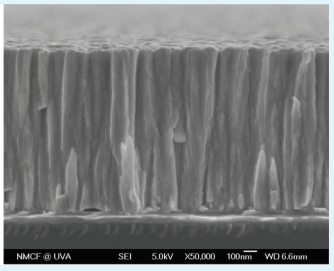


**KEYWORDS:** electrodeposition of alloys, hard magnetic films, magnetic anisotropy, Co−Pt, XPS valence band, electronic structure calculations, density functional theory

Co−Pt films with composition around Pt 25 at% grown by evaporation or sputtering exhibit a larger magnetocrystalline anisotropy (MCA) than that reported for bulk Co−Pt alloys in the same composition range.[1−3] The high anisotropy has been ascribed to the formation of a metastable phase with *Pmm*2 orthorhombic symmetry consisting of a hexagonal stacking of alternating atomic layers of pure Co and equiatomic Co−Pt, respectively. This phase is stabilized at intermediate growth temperatures (between 200 and 450 °C) by a balance between the surface diffusion of adsorbed atoms and the growth process due to the incoming flux of atoms. Enhanced diffusion favors the achievement of an equilibrium configuration, which involves Pt enrichment at the surface,[4] and thus facilitates the formation of Co/Pt bilayers; a high growth rate on the contrary favors kinetic trapping and the formation of random atomic mixtures.[5] To form the metastable phase, the growth temperature should be sufficiently high to enable a fraction of the Pt to be at the surface during growth, but not so high for diffusion processes to smear the atomic layering.

The magnetic anisotropy of these films has been observed to be along the vertical *c*-axis and to increase linearly with the volume fraction of ordered *Pmm*2 phase, extrapolating to $K_u \sim 3$ MJ/m$^3$ for the completely ordered phase.[3,6,7] Such phase and the corresponding synthesis conditions are therefore of extreme interest in the pursuit of magnetic media with high anisotropy and/or permanent magnet materials obtained by thin films processes.[8] Particularly useful is the possibility to synthesize such phase by electrochemical deposition. Due to its selective growth onto electrically conductive surfaces this technique is in fact capable to precisely reproduce deep sub-$\mu$m and high aspect ratio lithographic templates through a purely additive process, avoiding shadowing effects and etching defects usually seen with vacuum deposition techniques.[9]

In this Letter, we report on the observation of an unusually high MCA in electrodeposited Co-rich Co−Pt alloys. Comparison of experimental X-ray photoelectron spectra with electronic structure calculations based on density functional theory supports the hypothesis of formation of a *Pmm*2 phase in electrodeposited films.

Co-rich Co−Pt films were grown onto Au underlayers with a (111) preferred orientation, obtained by sputtering a bilayer Au(100 nm)/Cr(10 nm) on the native oxide of Si wafers or on glass. The Co−Pt films (Co ∼72−76 at %; P 3 at %; O ∼3 at%; Pt balance, as measured by X-ray photoelectron spectroscopy[10])

**Received:** March 3, 2011
**Accepted:** May 26, 2011
**Published:** May 26, 2011

 © 2011 American Chemical Society 

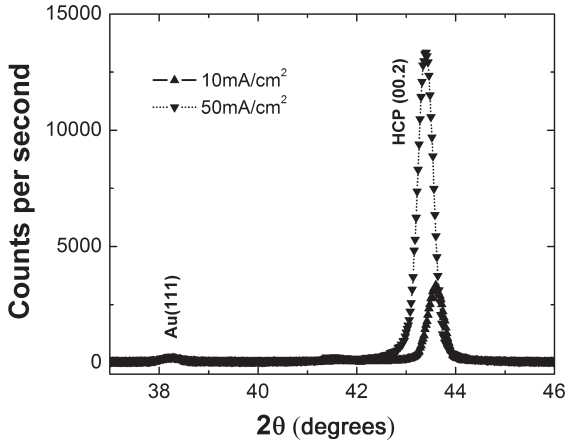


**Figure 1.** XRD patterns for 500 nm thick electrodeposited Co−Pt films grown on Au underlayers.

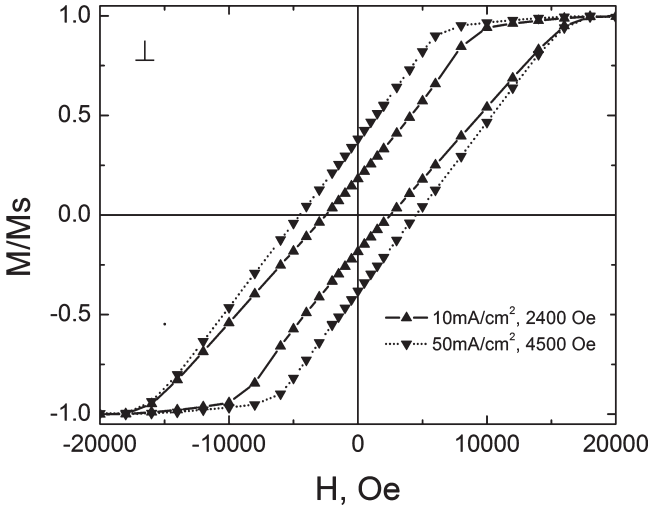


**Figure 2.** Perpendicular hysteresis loops of Co−Pt (Pt ~20 at%) films, 500 nm thick.

were electrodeposited at a current density (CD) of 10−50 mA/cm$^2$ from an amino-nitrite/citrate/glycine electrolyte containing 10 mM $Pt^{2+}$ and 0.1 M $Co^{2+}$, at a temperature of 75 °C, without solution stirring.[10,11]

Figure 1 shows the X-ray diffraction (XRD) patterns of 500 nm thick Co−Pt films electrodeposited onto Au substrates. The films are highly oriented according to a high-density plane that we identify as the hexagonal (00.2) plane.[12] The quality of the orientation is enhanced by increasing the current density, and the peak shifts to lower angles, indicating a slight increase in the Pt fraction (see Supporting Information for a discussion of these results). Figure 2 shows the magnetic hysteresis loops in the perpendicular direction for these films. The magnetic response suggests perpendicular anisotropy, with the loops being sheared because of a shape anisotropy contribution of the same order of magnitude as the MCA. Coercivity increases with current density and Pt content, and is probably related to the smaller grain size and magnetic decoupling at grain boundaries.[12] In-plane hysteresis loops (see Figure 2 in Supporting Information) evidence a linear response and a practically closed loop up to saturation. The almost ideal perpendicular response allows using the in-plane susceptibility to indirectly estimate the anisotropy of the films. In this method, for an oriented hexagonal film with the *c*-axis perpendicular to the surface, in-plane magnetization occurs against the MCA, and saturation ideally occurs at the field:

$$H_{sat} = 2K_{eff}/M_{sat} \quad (1)$$

where $K_{eff}$ is the effective anisotropy and $M_{sat}$ the saturation magnetization. $K_{eff}$ represents a lower bound estimate of the real anisotropy $K_u$ due to the thin film demagnetizing effect.

The maximum possible shape anisotropy, when the film is uniformly magnetized in the perpendicular direction, is $K_{shape} = 1/2\ M_{sat}^2$. An upper bound estimate for the anisotropy is therefore:

$$K' = K_{eff} + 1/2M_{sat}^2 \quad (2)$$

$K_{eff}$ was experimentally determined by linear extrapolation of the in-plane susceptibility observed at low fields to the saturation magnetization, and $M_{sat}$ was determined experimentally from the measured film moment and volume. The corresponding lower and upper bounds for $K_u$ obtained from eqs 1 and 2, respectively, are reported in Table 1; these values should be compared with the anisotropy values measured for bulk Co−Pt (Pt 20 at %) samples, estimated at 0.9−1 MJ/m$^3$.[3,13]

**Table 1. $K_{eff}$ and $K'$ (see text) for Electrodeposited Co-rich Co−Pt Films. $K_{eff}$ is Determined by In-plane Susceptibility Measurements and $K'$ is estimated from $K_{eff}$ and the Shape Anisotropy**

| CD (mA/cm$^2$) | $K_{eff}$ (MJ/m$^3$) | $K'$ (MJ/m$^3$) |
|---|---|---|
| 10 | 0.88 | 1.51 |
| 50 | 0.99 | 1.62 |

The intrinsic anisotropy $K_u$ expected in electrodeposited films should therefore be higher than the bulk value,[3,13] suggesting that a certain volume fraction of a high anisotropy phase might be present in electrodeposited films. Possible phases being formed in Co-rich Co−Pt include the disordered face-centered cubic, the ordered $L1_2$, the hexagonal close-packed $DO_{19}$, and the orthorhombic *Pmm*2 discussed above. Willoughby et al.[14] discuss the relative stability of the $L1_2$, $DO_{19}$ and *Pmm*2 phases, finding that the $L1_2$ phase is the most stable; however, the energy of the other two phases is only slightly higher (28−34 meV/at). Additionally, these differences in energy among the various phases decrease further if the structures are stretched. At the Au(111)/Co−Pt(00.2) interface the lattice mismatch is 12%, suggesting the possibility that epitaxy at such interface might decrease these energy differences.

There is no clear evidence of an ordered phase in our films. Extensive TEM investigations in this direction[12] were unsuccessful, and X-ray diffraction patterns (Figure 1) do not show any superlattice (00.1) peaks, which should be observed in case the *Pmm*2 phase were present in a significant amount. This, however, does not rule out the presence of such a phase, because a slight misalignment or a very small grain size of the ordered phase would fail to provide any significant X-ray signal.

To achieve a better insight into the crystal structure of electrodeposited films, we performed valence band X-ray photoelectron spectroscopy (XPS) measurements and we interpreted them by band structure calculations of the *Pmm*2, $DO_{19}$, and $L1_2$ phases.

Valence band and core level spectra of the Co−Pt alloys were investigated by XPS, using a PHI 5600 ESCA System, equipped with a hemispherical electron energy analyzer and an Al $K_\alpha$ monochromatic source (1486.6 eV).

All spectra were acquired at a takeoff angle of 45° with a pass energy of 2.95 eV and a resolution of 0.025 eV/step. The C1*s* core line (284.5 eV) was taken as the reference peak after Ar ion sputtering of the adventitious carbon surface layer. Sputtering of a 30 nm thick layer ($SiO_2$/Si calibration) was achieved using a 4 KeV beam voltage, 15 mA emission current, over a 4 × 4 $mm^2$ rastering area.

The electronic density of states (DOS) of $Co_3Pt$ alloys in the three phases were calculated within the density functional theory (DFT) by including self-consistently the spin−orbit interaction. We employed ultrasoft pseudopotentials,[15] a plane wave expansion of Kohn−Sham orbitals and the Perdew−Becke−Ernzerhof[16] approximation for the exchange and correlation energy as implemented in the Quantum ESPRESSO suite of programs.[17] Further details on the computational framework and on the resulting electronic properties are given in the Supporting Information.

The theoretical DOS of the *Pmm*2 phase together with other $Co_3Pt$ phases are reported in Figure 3a. By projecting the DOS on atomic pseudowave functions we estimated an electron transfer of 0.06−0.07$e^-$ from Pt to Co for all phases. This finding is in agreement with the interpretation of XANES spectra of pure Co, Pt and Co−Pt alloys by Lee et al.[18] who also reported Pt $4f_{7/2}$ and Co $2p_{3/2}$ core levels shifts for Co−Pt alloys similar (about 0.25 eV and −0.1 eV) to those we measured for the electrodeposited films at similar compositions. In our films the Pt $4f_{7/2}$ and Co $2p_{3/2}$ core levels are shifted with respect to the pure metals at higher (0.42 eV) and lower (− 0.075 eV) binding energies, respectively. As opposed to the interpretation of the core level shift in Co−Pt alloys given by Wakisaka et al.,[19] the sign of the charge transfer emerged from the ab initio calculation suggests that the positive shift of the Pt $4f_{7/2}$ level should be due to a lower screening at the Pt site in the alloys with respect to the pure phase. On the other hand the electron transfer from Pt to Co results in a positive shift (higher binding energy) of the valence bands projected on Co (cfr. Figure 5 in the Supporting Information) with respect to pure Co. The measured (small) negative shift of the Co $2p_{3/2}$ core level might thus be a result of electronic relaxation in the final state.

In Figure 3b, the experimental valence band photoemission spectrum of a Co−Pt film is compared with the theoretical spectra of the *Pmm*2 phase with and without the Shirley background correction. The theoretical photoemission spectra are obtained from the projections of the DOS on the two atomic species which were then weighed by the sensitivity factor $S_{Pt}/S_{Co}$ = 2.877 to account for the difference in the photoemission cross section of the two atomic species. To compare with experimental data, we convoluted the theoretical spectra with a Gaussian (variance 1 eV). Calculations of the photoemission spectra of pure metals show a good agreement with experiments in the position of the peaks with sizable misfit in the relative intensity presumably due to approximated transition matrix elements (cfr. Figure 6 in the Supporting Information). Comparison with experiments for the *Pmm*2 alloy is similarly good for peak positions and less satisfactory for intensities. The disagreement is, however, worse for the pure $L1_2$ and $DO_{19}$ phases or a mixture of the two. The photoemission spectra of the $Co_3Pt$ phases are also very different from the weighed superposition of the spectra of the two pure metals (cfr. Figure 7 in the Supporting Information).

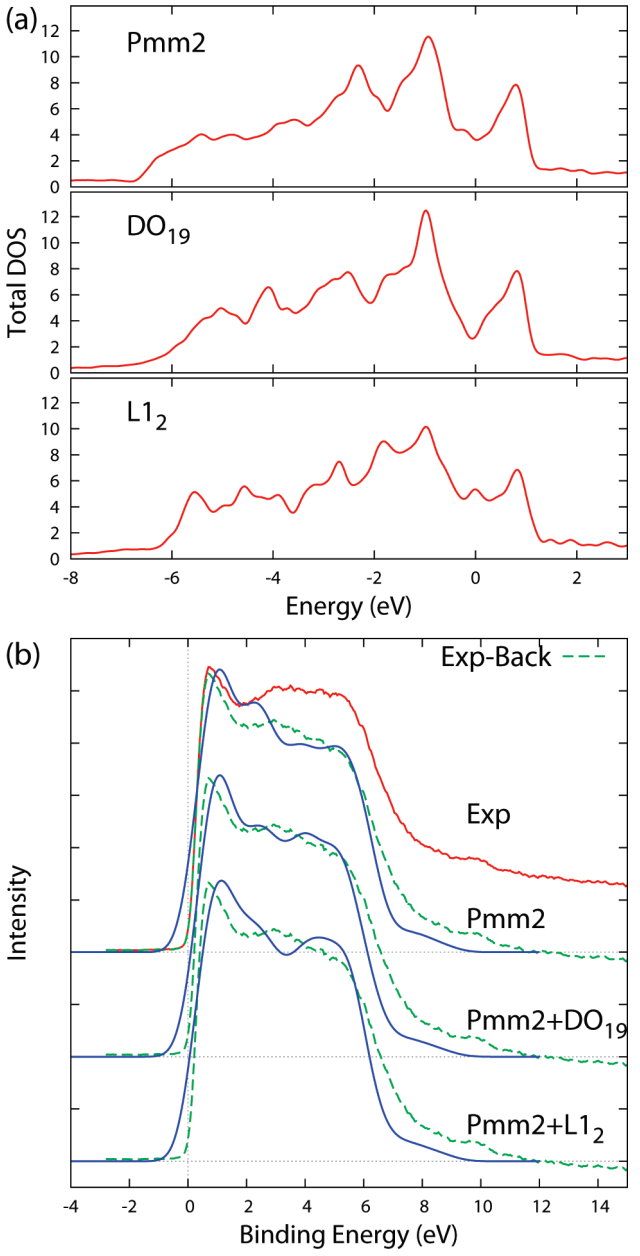


**Figure 3.** (a) Theoretical electronic density of states of the *Pmm*2, $DO_{19}$, and $L1_2$ phases. (b) Experimental photoemission spectrum (as recorded and with the background correction according to Shirley) compared with the theoretical spectra of the *Pmm*2 and of a mixture (50%−50%) of *Pmm*2 and $DO_{19}$ phases or of *Pmm*2 and $L1_2$ phases.

A better agreement with the experimental spectrum of the alloy is achieved by assuming a hypothetical mixture of the *Pmm*2 and the $DO_{19}$ phases, or to a lesser extent of the *Pmm*2 and the cubic $L1_2$ phases (Figure 3b, see the Supporting Information for further details). This outcome supports the notion that the electrodeposited films might indeed consist of a fraction of the *Pmm*2 phase mixed with one or both of the other two phases. The hypothesized structure would also explain the high anisotropy values observed.

In summary, electrodeposited Co-rich Co−Pt films exhibit a magnetocrystalline anisotropy larger than the corresponding bulk value and similar to that of films deposited by evaporation

or sputtering. A comparison of valence band XPS data with DFT predictions support the hypothesis that a certain volume fraction of the alloy may consist of the highly anisotropic *Pmm*2 phase, directly observed by others in films sputtered at relatively high temperatures.

## ■ ASSOCIATED CONTENT

**Supporting Information.** Information on electrodeposition process, computational details, and additional ab initio data. This material is available free of charge via the Internet at http://pubs.acs.org/.

## ■ AUTHOR INFORMATION

**Corresponding Author**
*E-mail: gz3e@virginia.edu.

**Present Addresses**
[||]Now at Seagate Technology, 7801 Computer Avenue South, Bloomington, MN 55435, USA
[#]Now at CNR, National Research Council of Italy, ISTM, Via Golgi 19, 20133 Milano, Italy

## ■ ACKNOWLEDGMENT

X.X. and G.Z. gratefully acknowledge financial support through NSF Grant DMR0705042.

## ■ REFERENCES

(1) Harp, G. R.; Weller, D.; Rabedeau, T. A.; Farrow, R. F. C.; Toney, M. F. *Phys. Rev. Lett.* **1993**, *71*, 2493–2496.
(2) Maret, M.; Cadeville, M. C.; Herr, A.; Poinsot, R.; Beaurepaire, E.; Lefebvre, S.; Bessière, M. *J. Magn. Magn. Mater.* **1999**, *191*, 61–71.
(3) Yamada, Y.; Suzuki, T.; Kanazawa, H.; Österman, J. C. *J. Appl. Phys.* **1999**, *85*, 5094–5096.
(4) Marković, N. M.; Ross, P. N., Jr. *Surf. Sci. Rep.* **2002**, *45*, 117–229.
(5) De Santis, M.; Baudoing-Savois, R.; Dolle, P.; Saint-Lager, M. C. *Phys. Rev. B* **2002**, *66*, 085412.
(6) Yamada, Y.; Suzuki, T.; Abarra, E. N. *IEEE Trans. Magn.* **1997**, *33*, 3622–3624.
(7) Yamada, Y.; Suzuki, T.; Abarra, E. N. *IEEE Trans. Magn.* **1998**, *34*, 343–345.
(8) Klemmer, T.; Hoydick, D.; Okumura, H.; Zhang, B.; Soffa, W. A. *Scripta Metall. Mater.* **1995**, *33*, 1793–1805.
(9) Zangari, G. Micro-electromechanical systems. In *Modern Electroplating*; Schlesinger, M., Ed.; Wiley: New York, 2010; Chapter 28.
(10) Pattanaik, G.; Kirkwood, D. M.; Xu, X.; Zangari, G. *Electrochim. Acta* **2007**, *52*, 2755–2764.
(11) Pattanaik, G.; Zangari, G.; Weston, J. *Appl. Phys. Lett.* **2006**, *89*, 112506.
(12) Zana, I.; Zangari, G.; Shamsuzzoha, M. *J. Magn. Magn. Mater.* **2005**, *292*, 266–280.
(13) Bolzoni, F.; Leccabue, F.; Panizzieri, R.; Pareti, L. *IEEE Trans. Magn.* **1984**, *20*, 1625–1627.
(14) (a) Willoughby, S. D.; Stern, R. A.; Duplessis, R. R.; MacLaren, J. M.; McHenry, M. E.; Laughlin, D. E. *J. Appl. Phys.* **2003**, *93*, 7145–7147.(b) MacLaren, J. M.; Duplessis, R. R.; Stern, R. A.; Willoughby, S. D. *IEEE Trans. Magn.* **2005**, *41*, 4374−4379.
(15) Vanderbilt, D. *Phys. Rev. B* **1990**, *41*, 7892–7895.
(16) Perdew, J. P.; Burke, K.; Erznerhof, M. *Phys. Rev. Lett.* **1996**, *77*, 3865.
(17) Giannozzi, P.; Baroni, S.; Bonini, N.; Calandara, M.; Car, R.; Cavazzoni, C.; Ceresoli, D.; Chiarotti, G. L.; Cococcioni, M.; Dabo, I.; Corso, A. D.; de Gironcoli, S.; Fabris, S.; Fratesi, G.; Gebauer, R.; Gerstmann, U.; Gougoussis, C.; Kokalj, A.; Lazzeri, M.; Martin-Samos, L.; Marzari, N.; Mauri, F.; Mazzarello, R.; Paolini, S.; Pasquarello, A.; Paulatto, L.; Sbraccia, C.; Scandolo, S.; Sclauzero, G.; Seitsonen, A. P.; Smogunov, A.; Umari, P.; Wentzcovitch, R. M. *J. Phys. Chem. B* **2006**, *110*, 23489–23496.
(18) Lee, Y.-S.; Lim, K.-Y.; Chung, Y.-D.; Whang, C.-N.; Jeon, Y. *Surf. Interface Anal.* **2000**, *30*, 475–478.
(19) Wakisaka, M.; Mitsui, S.; Hirose, Y.; Kawashima, K.; Uchida, H.; Watanabe, M. *J. Phys. Chem. B* **2006**, *110*, 23489–23496.